Supplementary Information

Modular Assembly of Electron Transfer Pathway in Bimetallic MOF for Photocatalytic Ammonia Synthesis

Ke An[a, b‡], *Jiangdan Tan*[a, b‡], *Dong Yang*[c, d]*, *Hanjie Ren*[a, b], *Zhanfeng Zhao*[a, b], *Yao Chen*[a, b], *Wenjing Wang*[a, b], *Xin Xin*[a, b], *Yonghui Shi*[a, b] *and Zhongyi Jiang*[a, b, e]*

[a] Key Laboratory for Green Chemical Technology of Ministry of Education, School of Chemical Engineering and Technology, Tianjin University, Tianjin 300072, China

[b] Collaborative Innovation Center of Chemical Science and Engineering (Tianjin), Tianjin 300072, China

[c] Key Laboratory of Systems Bioengineering of Ministry of Education, School of Chemical Engineering and Technology, Tianjin 300072, China

[d] School of Environmental Science and Engineering, Tianjin University, Tianjin 300072, China

[e] Joint School of National University of Singapore and Tianjin University, International Campus of Tianjin University, Binhai New City, Fuzhou, 350207, China

* Corresponding authors: Dong Yang (dongyang@tju.edu.cn); Zhongyi Jiang (zhyjiang@tju.edu.cn)

‡ Ke An and Jiangdan Tan contributed equally to the work.

CONTENT

1. Supporting Experimental Section

1.1. Chemicals

Hafnium (IV) tetrachloride ($HfCl_4$, ≥99.5%) was purchased from Macklin Biochemical Reagent Co., Ltd. (Shanghai, China). Ceric (IV) ammonium nitrate ($(NH_4)_2Ce(NO_3)_6$, ≥99.5%) and 2-aminoterephthalic acid (TPA-NH_2, ≥98%) were obtained from Heowns Biochemical Technology Co., Ltd. (Tianjin, China). N, N-dimethylformamide (DMF, ≥99.9%), methanol (MeOH, ≥99.5%), acetic acid (HAc, ≥99.7%) and dimethyl sulfoxide-d_6 (DMSO-d_6) were received from Aladdin Chemistry Co. Ltd (Shanghai, China). Potassium sulfite (K_2SO_3, ≥98%) was bought from Energy Chemical (Shanghai, China). All chemicals were used without further purification.

1.2. Electrochemical Measurements

The photocurrent response and electrochemical impedance spectra (EIS) of photocatalysts were conducted by the electrochemical experiments on a CHI660D electrochemical workstation. A three-electrode system consisting of a reference electrode (Ag/AgCl), a counter electrode (Pt foil) and a working electrode was constructed, and Na_2SO_4 solution (0.1 mol L^{-1}) was employed as the electrolyte. The preparation process of the working electrode was as below: 10 mg photocatalyst was dispersed in 1 mL of aqueous Nafion solution (10 vol%), and then the suspension was ultrasonically treated for 20 min. Thereafter, the suspension was dripped on the surface of a 1 × 2 cm^2 fluorine-doped tin oxide (FTO) glass, which was subsequently placed in a 40 °C oven all night. In the EIS Nyquist plot and transient photocurrent, initial voltage, alternating voltage and frequency were -0.1 V, 5 mV and 10^5-10^{-2} Hz, respectively. A 300 W xenon lamp was applied as the illuminant.

1.3. Nitrogen-Reduction Apparent Quantum Efficiency Measurements

For measurement of the Nitrogen-Reduction Apparent Quantum Efficiency (AQE), the N_2 photofixation reaction was carried out under monochromatic light using bandpass filters (center wavelengths: 380, 405, 420, 450 and 500 nm, full width at half maximum for all: 20 nm, Beijing China Education Au-light Co., Ltd.). The

corresponding power density was measured using an optical power meter (CEL-NP2000). The AQE was calculated according to the following equation

$$\text{AQE}(\%)= \frac{3 \times \text{the number of the generated ammonia molecules}}{\text{number of the incident photons}} \times 100\%$$

To determine the AQE, the reactions were carried out in a sealed photocatalytic reactor under monochromatic light irradiation. The photocatalyst (10 mg) was dispersed in pure water (100 mL) 79 mg potassium sulfite (K_2SO_3) reagent. Next, the nitrogen was flowed into the mixed solution with the rate of 60 mL min-1. After stirring continuously in the dark for 0.5 h, the reactor was irradiated by the xenon lamp and 2 mL reaction solution was taken every 0.5 h to determine the ammonia concentration by ion chromatography.

1.4. $^{15}N_2$ isotope labelling experiments

The $^{15}N_2$ isotope labelling experiments were measured *via* nuclear magnetic resonance (NMR) method (Varian Inova, 500 MHz, USA). First, 5 mL reaction liquid was filtrated by a 0.22 μm membrane to remove solid catalysts. Afterwards, the obtained solution was adjusted by 6 mol L^{-1} H_2SO_4 solution to pH=1.2. Finally, add 100 mL DMSO-d_6 to 1 mL acidized solution and mix adequately.

1.5. Photocatalytic H_2 Evolution Experiment

Photocatalytic H_2 evolution rates of all prepared samples were determined in a Pyrex top-irradiation reaction vessel under full spectrum. The light source was a CEL-HXF300 300 W xenon lamp (Ceaulight, Beijing). 10 mg samples were suspended in 100 mL water and 79 mg K_2SO_3 was added as the sacrificial agent. The reactor was vacuumed to remove the dissolved O_2 before the light irradiation. Every 0.5 h, the produced gas was fetched from the photocatalytic reactor and injected in a TechcompGC7900 gas chromatography (equipped with TCD) to analyze the H_2 yield.

2. Characterization Methods

The morphology and microstructure of NU6(Ce-Hf) samples were reflected by the scanning electron microscopy (SEM, Hitachi S-4800, Japan) and transmission electron microscopy (TEM, JEOL JEM-2100F). The characteristic peaks of crystal

structure were recorded through X-ray powder diffraction (XRD) patterns using Rigaku D/max 2500 V/PC X-ray diffractometer. Fourier transform infrared spectroscopy (FTIR) of photocatalysts was performed by adopting a Nicolet-560 Fourier transform infrared spectrometer. The specific surface area was measured by using TRISTAR-3000 surface area analyzer (USA) at 77 K and calculated by the Brunauer-Emmett-Teller (BET) method. Thermogravimetric analysis (TGA) was conducted on a Perkin-Elmer TG/DTA thermo-gravimetric analyzer by heating from 40 to 800 ^{o}C at a rate of 10 ^{o}C min^{-1} in N_2 atmosphere. Photoluminescence (PL) fluorescence spectra were conducted by a Jobin Yvon Fluorolog3-21 fluorescence spectrometer. The UV-vis diffuse reflection spectra (DRS) of photocatalysts were acquired by a Hitachi U-3010 UV-vis spectrophotometer. The controlled experiments under different gas atmospheres were measured *via* the nuclear magnetic resonance (NMR) method (Varian Inova, 500 MHz, USA). The reaction solution was measured by ion chromatography (IC, Thermo ICS-600, USA) to determine the ammonia concentration.

3. Theoretical Calculations

Density functional theory (DFT) simulations were performed to calculate the electronic properties and N_2 activation with Cambridge Sequential Total Energy Package (CASTEP) software in Materials Studio 2018. The calculated lattice parameters for primary unit cell of NU6(Ce-Hf) with 3 Ce, 3 Hf, 48 C, 6 N, 32 O and 42 H atoms are a = 14.50 Å, b = 14.32 Å, c = 14.56 Å, and $\alpha = 59.98^{o}$, $\beta = 59.79^{o}$, $\gamma = 59.70^{o}$, which was modified by the unit cell of the literature.[1-3] Both of molecular structures were consistent with the actual situation of the experiments (**Fig. S10** and **Table S7**). All structures were optimized by the Forcite module with Universal Force Field (UFF) and the CASTEP software package for the first principles was exploited for DFT calculation in this work.[4] As for the Forcite module, the energy convergence tolerance was 2×10^{-5} kcal mol^{-1}, the force convergence tolerance was 1×10^{-3} kcal mol^{-1} Å^{-1}, the stress convergence tolerance was 1×10^{-3} GPa, and the displacement convergence tolerance was 1×10^{-5} Å, respectively. As for the CASTEP software

package, the electron exchange and correlation were described by the hybrid density functional (B3LYP), which can further improve the bandgap accuracy and extremely versatile compared with Local Density Approximations (LDA) and Generalized Gradient Approximations (GGA).[5-7] The cut-off energy was fitted to 500 eV with plane-wave basis. The Brillouin zone was sampled with $1 \times 1 \times 1$ k-point for structural optimization and calculation. Geometry optimization was accomplished before the energy calculation. A supercell with two layers was used as a support to model the NU6(Ce-Hf) (111) surface, while the top layer was allowed to relax and the bottom layer was constrained. The vacuum region was set to prevent the interaction between two neighboring layers.

The grand canonical Monte Carlo (GCMC) for Sorption module was used to simulate the adsorption process and distribution plots of N_2 molecules with Universal Force Field (UFF). The N_2 adsorption of NU6(Ce-Hf) model was simulated at 298 K from 0 to 101.3 kPa. The method was set to metropolis, while the equilibration steps and production steps were adjusted to 10^7.

Additionally, because of the calculation complexity and relative limitation of CASTEP in the calculation, the models do not describe the interactions and structural changes between units, while they are not optimized over spin states and transition state barriers were not included. Thus, the models were only intended to give qualitative analysis.

4. Supporting Data

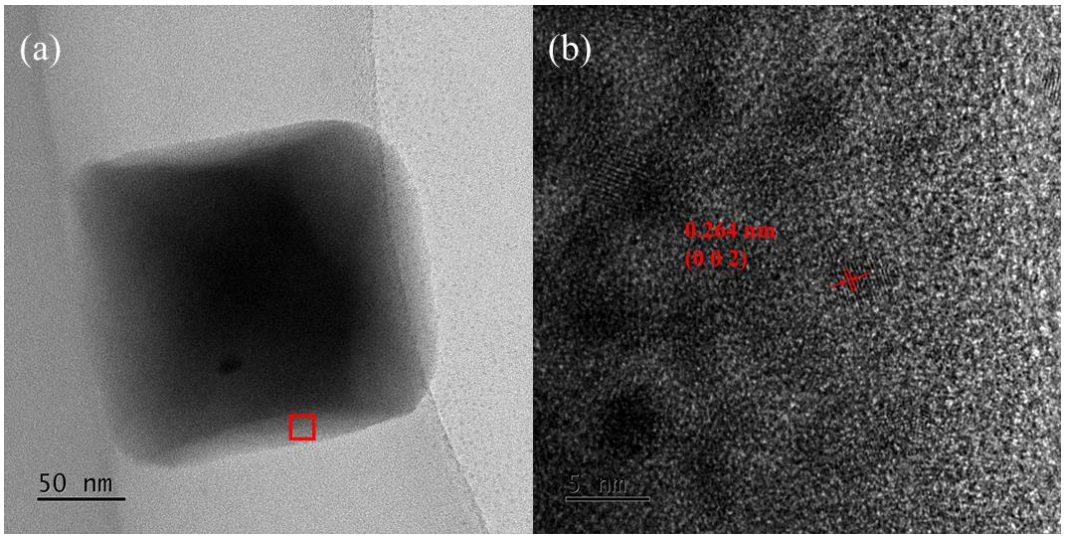

Fig. S1 (a) TEM and (b) HRTEM (red area in a) of NU6(1Ce-1Hf) samples.

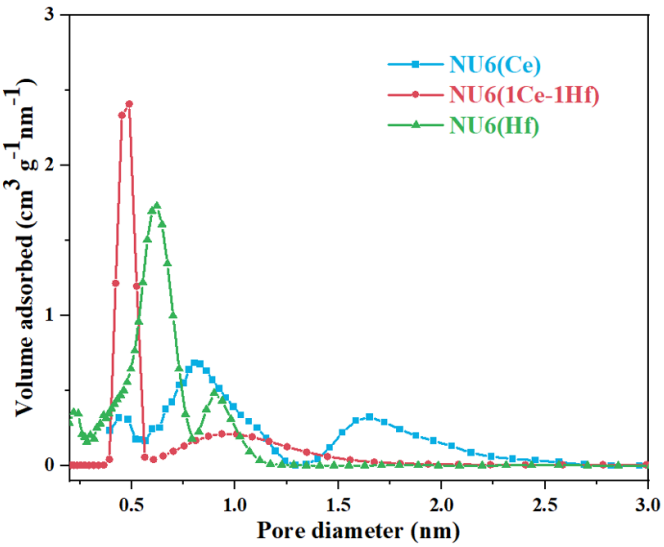

Fig. S2 Barrett-Joyner-Halenda (BJH) pore-size distribution curves of NU6(Ce), NU6(1Ce-1Hf) and NU6(Hf).

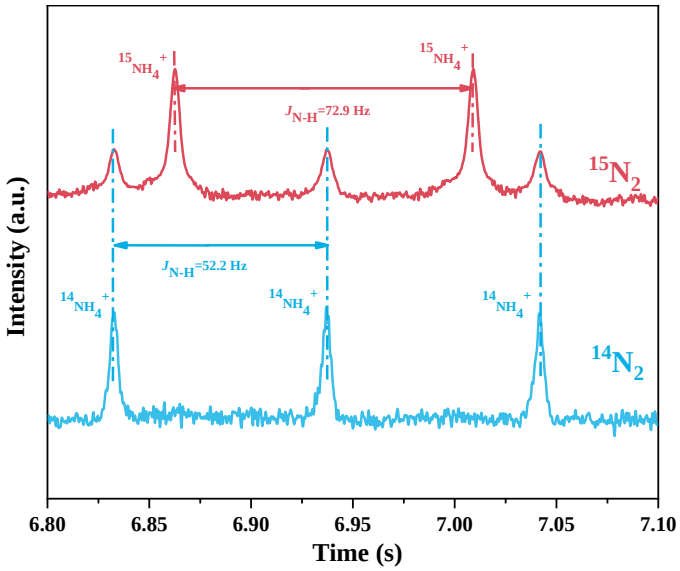

Fig. S3 ^1H NMR (500 MHz) spectra of photocatalytic N_2 fixation reaction solutions over NU6(1Ce-1Hf) in different gas atmospheres.

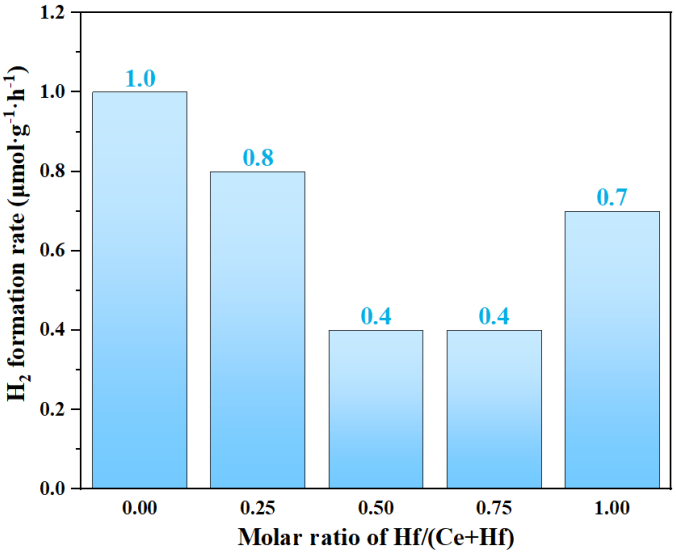

Fig. S4 H_2 evolution rates over all NU6(Ce-Hf) samples under full spectrum.

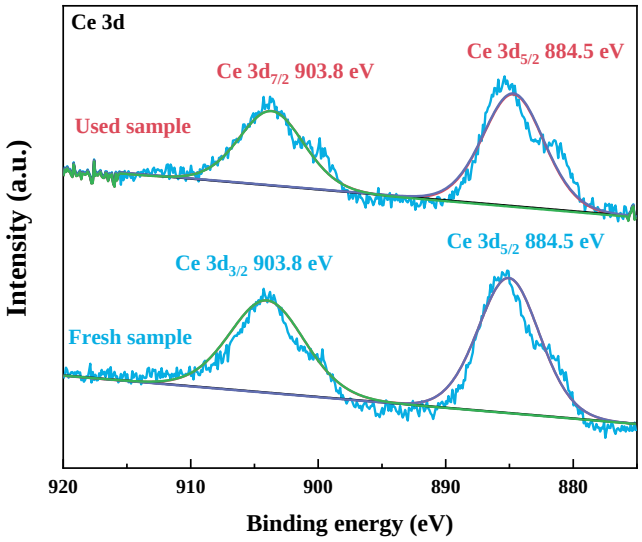

Fig. S5 XPS spectra of Ce 3d over NU6(1Ce-1Hf) before and after the stability test.

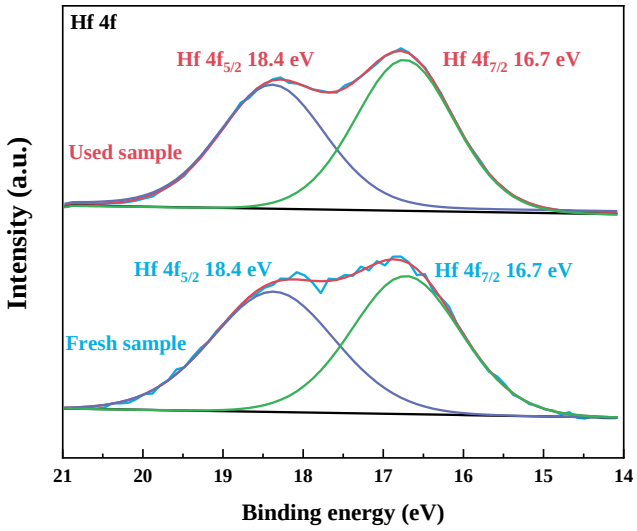

Fig. S6 XPS spectra of Hf 4f over NU6(1Ce-1Hf) before and after the stability test.

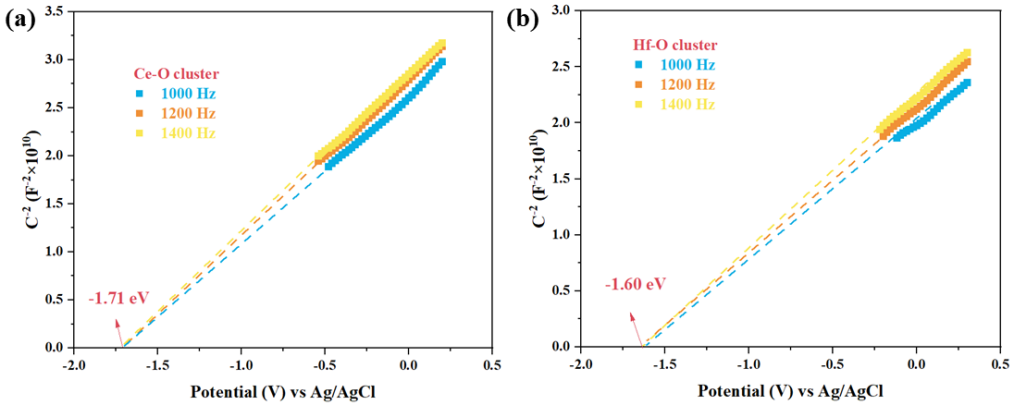

Fig. S7 Mott-Schottky plots of (a) the Ce-O and (b) Hf-O cluster.

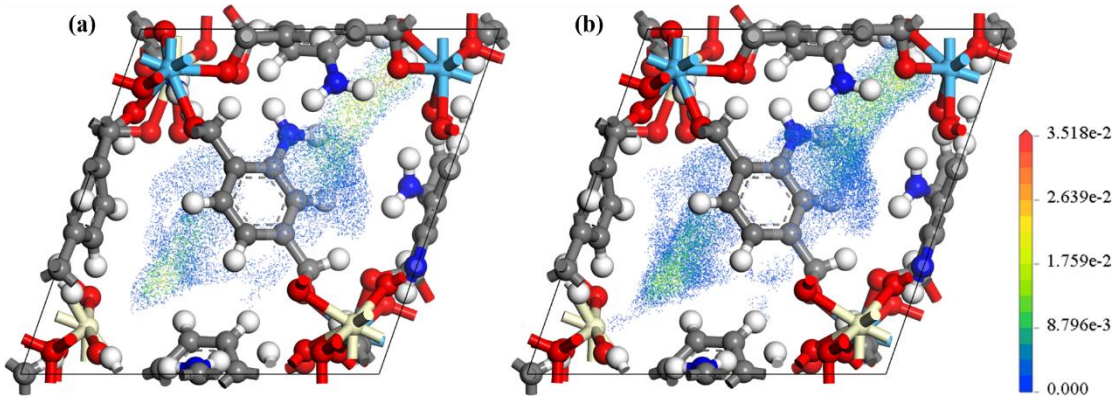

Fig. S8 Probability distribution plots of (a) N_2 molecules and (b) N_2 and H_2O molecules in the adsorption of NU6(Ce-Hf) at 298 K simulated by the GCMC method. Key: yellow balls, Ce; light blue balls, Hf; grey balls, C; dark blue balls, N; red balls: O; white ball, H.

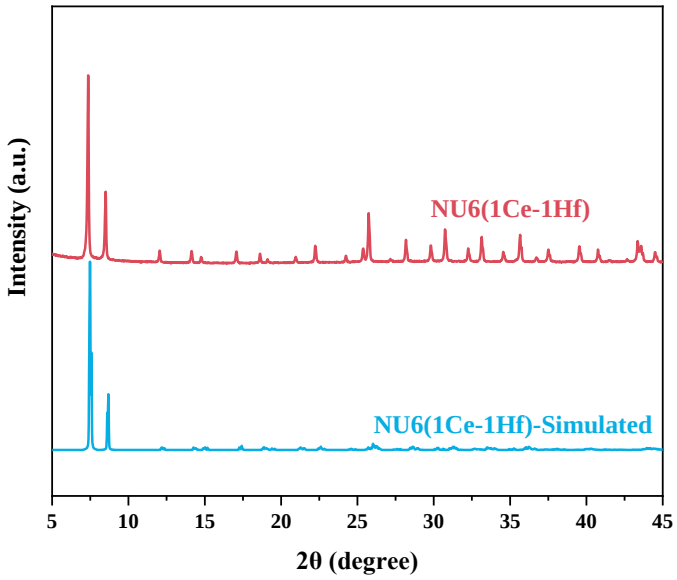

Fig. S9 XRD patterns of NU6(1Ce-1Hf) and NU6(1Ce-1Hf)-Simulated.

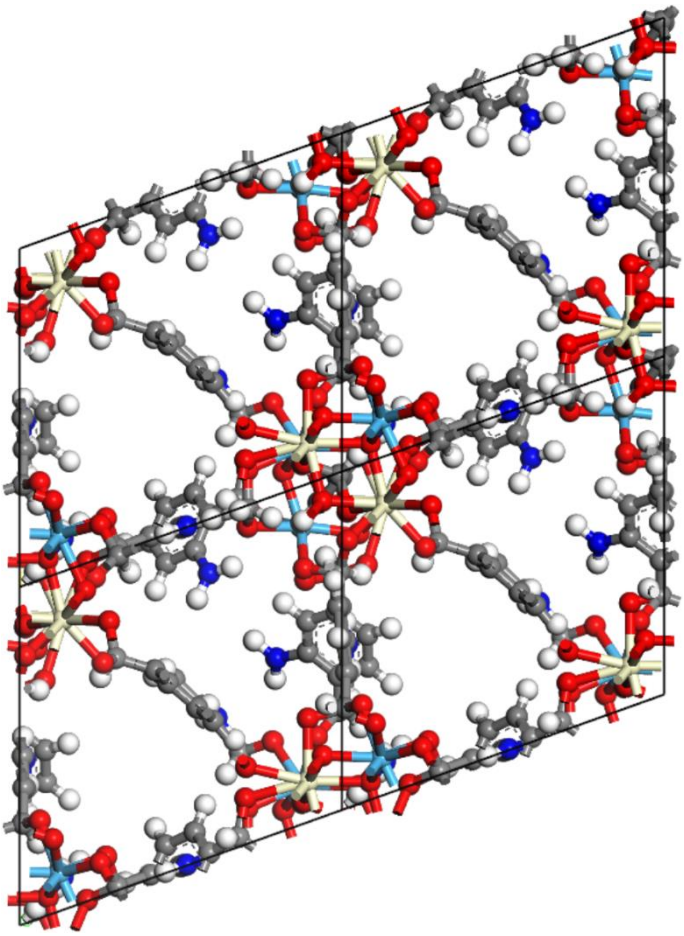

Fig. S10 Schematic diagrams of NU6(Ce-Hf) unit cells. Key: yellow balls, Ce; light blue balls, Hf; grey balls, C; dark blue balls, N; red balls: O; white ball, H.

5. Tables

Table S1 The actual and theoretical Ce/Hf molar ratio of NU6(Ce), NU6(1Ce-1Hf) and NU6(Hf).

Photocatalyst	**Actual molar ratio*** **(Ce: Hf)**	**Theoretical molar ratio (Ce: Hf)**
NU6(Ce)	1.00: 0	1.00: 0
NU6(1Ce-1Hf)	1.16: 1.00	1.00: 1.00
NU6(Hf)	0: 1.00	0: 1.00

* The values are calculated by the ICP-OES data.

Table S2 The BET specific surface area, nitrogen adsorbed volume and pore diameter of NU6(Ce), NU6(1Ce-1Hf) and NU6(Hf).

Photocatalyst	Adsorbed volume ($cm^3\ g^{-1}$)	Pore diameter (nm)	S_{BET} ($m^2\ g^{-1}$)
NU6(Ce)	179.5	1.1	676.0
NU6(1Ce-1Hf)	216.1	0.9	779.7
NU6(Hf)	202.5	0.5	663.8

Table S3 The absorption edge, band gap, conduction band and valence band potential of all NU6(Ce-Hf) samples.

Photocatalyst	Absorption edge (nm)	E_g (eV)	E_{cb} (eV)	E_{vb} (eV)
NU6(Ce)	452	2.76	-0.35	2.41
NU6(3Ce-1Hf)	450	2.75	-0.28	2.47
NU6(1Ce-1Hf)	447	2.72	-0.43	2.29
NU6(1Ce-3Hf)	444	2.80	-0.37	2.43
NU6(Hf)	441	2.82	-0.24	2.58

Table S4 Photocatalytic nitrogen fixation performance of MOF-based materials.

Catalyst	Light source	Detection method	NH_3 evolution rate/μmol $h^{-1}\ g^{-1}$	Reference
MIL-101(Fe)	Full spectrum	NR [a]	50.4	(8)
ZIF-67@PMo_4V_8	Full spectrum	NR [a]	149.0	(9)
Ti_3C_2-QD/Ni-MOF	Full spectrum	NR [a]	88.79	(10)
MOF-76(Ce)	Full spectrum	IB [b]	34.0	(11)
Al-PMOF(Fe)	≥420 nm	IB [b]	7.1	(12)
Ru-In_2O_3 HPNs	1 sun with AM1.5G filter	IB [b]	44.5	(13)
NH_2-MIL-125 (Ti)	≥400 nm	IC [c]	12.3	(14)
MIL-53 (Fe^{II}/Fe^{III})	≥420 nm	IC [c]	306	(15)

U(0.5Hf)-2SH	≥420 nm	IC [c]	116.1	(1)
NU6(1Ce-1Hf)	Full spectrum	IC [c]	158.4	This work

[a] The detection method of Nessler's reagent.

[b] The detection method of indophenol blue.

[c] The detection method of ion chromatography.

Table S5 Photocatalytic nitrogen fixation performance of different materials detected by the ion chromatography.

Catalyst	**Light source**	**NH_3 evolution rate/μmol h^{-1} g^{-1}**	**Reference**
NH_2-MIL-125 (Ti)	⩾400 nm	12.3	(14)
U(0.5Hf)-2SH	⩾420 nm	116.1	(1)
MIL-53(Fe^{II}/Fe^{III})	⩾420 nm	306.0	(15)
TiO_2	Full spectrum	324.8	(16)
g-C_3N_4	⩾420 nm	105.0	(17)
Cu_2O	⩾400 nm	30.3	(18)
Cu-TiO_2	200-800 nm	78.9	(19)
MoO_{3-x}	⩾300 nm	11.1	(20)
NU6(1Ce-1Hf)	Full spectrum	158.4	This work

Table S6 Calculated nitrogen-reduction apparent quantum efficiency over NU6 (1Ce-1Hf) at different wavelengths.

Wavelength λ(nm)	**Light power density I (mW cm^{-2})**	**Light power P (mW)**	**Ammonia generated (μmol h^{-1})**	**AQE (%)**
380	65	2156	54.0	0.65
405	54	1791	41.0	0.56
420	60	1990	9.6	0.11
450	72	2388	12.6	0.12
500	66	2189	9.2	0.08

Taking the λ=380 nm as an example,

The diameter of the reactor is 6.5 cm. The irradiation area of the solution is

$$S = \pi \times \left(\frac{\mathrm{d}}{2}\right)^2 = 3.14 \times (3.25)^2 = 33.17 cm^2 \quad (1)$$

The light power is

$$P = I \times S = 65 \times 33.17 = 2156\ mW \quad (2)$$

The number of the incident photons at 380 nm is

$$N_{incident} = \frac{Pt}{h\nu} = \frac{Pt\lambda}{hc} = \frac{2165 \times 10^{-3} \times 3600 \times 380 \times 10^{-9}}{6.63 \times 10^{-34} \times 3 \times 10^{8}} = 1.49 \times 10^{22} \quad (3)$$

In the above equation, P is the light power, t is the irradiation time (1 h = 3600 s), h is Planck's constant, ν is the light frequency, and c is the speed of light in free space.

The number of reacted electrons is

$$N_{reacted} = 3 \times \textit{the number of the generated ammonia molecules}$$

$$= 3 \times 54.0 \times 10^{-6} \times 6.02 \times 10^{23} = 9.75 \times 10^{19} \quad (4)$$

The AQE can be calculated as

$$AQE = \frac{N_{reacted}}{N_{incident}} \times 100\% = \frac{9.75 \times 10^{19}}{1.49 \times 10^{22}} \times 100\% = 0.65\% \quad (5)$$

Table S7 The coordinates of different atoms in the NU6(1Ce-1Hf) model.

Element	Atom number	Fractional coordinates of atoms		
		NU6(1Ce-1Hf)		
		u	v	w
H	1	0.33	1.02	0.50
H	2	0.15	0.49	1.03
H	3	0.68	-0.01	0.50

H	4	-0.13	0.89	0.52
H	5	0.58	0.42	0.85
H	6	0.45	0.60	0.12
H	7	0.42	0.14	0.85
H	8	-0.01	0.51	0.67
H	9	-0.02	0.69	0.50
H	10	0.58	0.16	0.85
H	11	1.03	0.32	0.50
H	12	0.42	0.85	0.15
H	13	1.11	0.07	0.30
H	14	0.42	0.59	0.85
H	15	-0.12	0.90	0.69
H	16	0.50	1.01	0.33
H	17	0.15	0.32	1.02
H	18	0.82	0.67	0.01
H	19	1.06	0.68	0.23
H	20	0.64	1.04	1.10
H	21	1.06	0.22	0.67
H	22	0.34	0.93	0.96
H	23	1.05	1.03	0.23
H	24	0.25	0.65	1.02
H	25	1.05	1.03	0.67
H	26	0.64	0.23	1.09
H	27	0.78	0.94	0.33
H	28	0.95	0.33	0.94
H	29	0.34	0.94	0.76
H	30	0.95	0.76	0.95
H	31	0.79	0.46	-0.04
H	32	0.73	0.59	-0.02
H	33	1.03	0.41	0.31
H	34	1.01	0.55	0.23
H	35	0.55	0.78	0.24
H	36	0.66	0.84	0.19
H	37	0.67	0.32	0.18
H	38	0.59	0.45	0.21
H	39	0.59	0.00	0.68
H	40	0.45	0.01	0.76
H	41	0.19	0.13	0.38
H	42	0.13	0.12	0.52
C	1	0.89	0.50	0.00
C	2	0.40	1.01	0.50
C	3	0.08	0.49	1.02
C	4	0.60	0.00	0.50
C	5	-0.07	0.93	0.51

C	6	0.55	0.46	0.91
C	7	1.07	0.04	0.48
C	8	0.48	0.56	0.06
C	9	0.45	0.08	0.92
C	10	1.01	0.50	0.40
C	11	0.54	0.92	0.09
C	12	0.00	0.51	0.60
C	13	-0.01	0.61	0.50
C	14	0.54	0.09	0.92
C	15	1.02	0.40	0.50
C	16	0.45	0.92	0.08
C	17	1.06	0.03	0.39
C	18	0.46	0.56	0.91
C	19	-0.07	0.93	0.60
C	20	0.57	0.46	0.07
C	21	0.50	1.00	0.41
C	22	0.08	0.40	1.02
C	23	0.51	0.00	0.59
C	24	0.89	0.60	0.01
C	25	-0.01	0.30	0.00
C	26	-0.01	0.40	0.00
C	27	0.30	0.01	0.70
C	28	0.41	0.01	0.60
C	29	-0.03	0.70	0.02
C	30	-0.02	0.59	0.02
C	31	0.71	-0.01	0.30
C	32	0.60	-0.01	0.40
C	33	-0.01	-0.01	0.30
C	34	-0.01	-0.02	0.40
C	35	0.68	0.28	0.01
C	36	0.60	0.40	-0.01
C	37	-0.01	-0.01	0.70
C	38	0.00	-0.01	0.59
C	39	0.30	0.69	0.02
C	40	0.42	0.61	-0.01
C	41	0.31	-0.01	0.00
C	42	0.41	0.00	0.00
C	43	-0.01	0.71	0.30
C	44	0.00	0.60	0.40
C	45	0.68	0.03	0.02
C	46	0.59	0.01	0.01
C	47	0.01	0.30	0.70
C	48	0.01	0.40	0.59
N	1	0.80	0.52	-0.02

N	2	1.13	0.10	0.46
N	3	1.02	0.48	0.31
N	4	0.59	0.84	0.18
N	5	0.61	0.41	0.16
N	6	0.52	0.00	0.69
O	1	0.92	0.24	0.11
O	2	0.21	1.00	0.70
O	3	0.08	0.70	1.02
O	4	0.71	0.11	0.24
O	5	0.02	0.88	0.30
O	6	0.70	0.23	0.93
O	7	0.88	0.06	0.74
O	8	0.26	0.69	0.13
O	9	0.25	0.10	0.93
O	10	0.88	0.75	0.29
O	11	0.78	0.93	0.01
O	12	0.06	0.29	0.76
O	13	0.02	0.79	0.30
O	14	0.70	0.14	0.94
O	15	0.89	0.31	0.76
O	16	0.23	0.95	0.11
O	17	0.88	0.06	0.29
O	18	0.28	0.80	0.94
O	19	0.02	0.88	0.78
O	20	0.79	0.28	0.00
O	21	0.71	0.94	0.24
O	22	0.10	0.22	0.97
O	23	0.27	0.11	0.73
O	24	0.89	0.72	0.12
O	25	0.05	0.05	0.06
O	26	0.09	0.05	0.80
O	27	0.05	0.80	0.06
O	28	0.82	0.06	0.05
O	29	0.94	0.94	0.17
O	30	0.94	0.93	0.94
O	31	0.94	0.18	0.94
O	32	0.20	0.92	0.93
Ce	1	0.13	0.86	0.87
Ce	2	0.13	0.87	0.11
Ce	3	0.90	0.12	0.86
Hf	1	0.87	0.12	0.12
Hf	2	0.12	0.11	0.88
Hf	3	0.87	0.88	0.12

6. References

1 K. An, H. Ren, D. Yang, Z. Zhao, Y. Gao, Y. Chen, J. Tan, W. Wang and Z. Jiang, *Appl. Catal., B*, 2021, **292**, 120167.

2 S. Oien, D. Wragg, H. Reinsch, S. Svelle, S. Bordiga, C. Lamberti and K. P. Lillerud, *Cryst. Growth Des.*, 2014, **14**, 5370-5372.

3 D. Banerjee, W. Xu, Z. Nie, L. E. V. Johnson, C. Coghlan, M. L. Sushko, D. Kim, M. J. Schweiger, A. A. Kruger, C. J. Doonan and P. K. Thallapally, *Inorg. Chem.*, 2016, **55**, 8241-8243.

4 S. J. Clark, M. D. Segall, C. J. Pickard, P. J. Hasnip, M. J. Probert, K. Refson and M. C. Payne, *Z. Kristallogr.*, 2005, **220**, 567-570.

5 G. U. von Oertzen, W. M. Skinner and H. W. Nesbitt, *Phys. Rev. B*, 2005, **72**, 235427.

6 H. Ren, D. Yang, F. Ding, K. An, Z. Zhao, Y. Chen, Z. Zhou, W. Wang and Z. Jiang, *J. Photochem. Photobiol. A-Chem.*, 2020, **400**, 112729.

7 J. Li, W. Zhao, J. Wang, S. Song, X. Wu and G. Zhang, *Appl. Surf. Sci.*, 2018, **458**, 59-69.

8 G. Li, F. Li, J. Liu and C. Fan, *J. Solid State Chem.*, 2020, **285**, 121245.

9 X.-H. Li, P. He, T. Wang, X.-W. Zhang, W.-L. Chen and Y.-G. Li, *ChemSusChem*, 2020, **13**, 2769-2778.

10 J. Qin, B. Liu, K.-H. Lam, S. Song, X. Li and X. Hu, *ACS Sustainable Chem. Eng.*, 2020, **8**, 17791-17799.

11 C. Zhang, Y. Xu, C. Lv, X. Zhou, Y. Wang, W. Xing, Q. Meng, Y. Kong and G. Chen, *ACS Appl. Mater. Interfaces*, 2019, **11**, 29917-29923.

12 S. Shang, W. Xiong, C. Yang, B. Johannessen, R. Liu, H. Y. Hsu, Q. Gu, M. K. H. Leung and J. Shang, *ACS Nano*, 2021, **15**, 9670-9678.

13 V. Manh-Hiep, Q. Toan-Anh and D. Trong-On, *Sustainable Energy Fuels*, 2021, **5**, 2528-2536.

14 H. Huang, X. Wang, D. Philo, F. Ichihara, H. Song, Y. Li, D. Li, T. Qiu, S. Wang and J. Ye, *Appl. Catal., B*, 2020, **267**, 118686.

15 Z. Zhao, D. Yang, H. Ren, K. An, Y. Chen, Z. Zhou, W. Wang and Z. Jiang, *Chem. Eng. J.*, 2020, **400**, 125929.

16 G. Zhang, X. Yang, C. He, P. Zhang and H. Mi, *J. Mater. Chem. A*, 2020, **8**, 334-341.

17 Y. Qi, Y. Chen, R. Wang, L. Wang, F. Zhang, Q. Shen, P. Qu and D. Liu, *Catal Letters*, 2021, **151**, 1546-1555.

18 S. Zhang, Y. Zhao, R. Shi, C. Zhou, G. I. N. Waterhouse, Z. Wang, Y. Weng and T. Zhang, *Angew. Chem. Int. Ed.*, 2021, **60**, 2554-2560.

19 Y. Zhao, Y. Zhao, R. Shi, B. Wang, G. I. N. Waterhouse, L.-Z. Wu, C.-H. Tung and T. Zhang, *Adv Mater*., 2019, **31**, 1806482.

20 Y. Li, X. Chen, M. Zhang, Y. Zhu, W. Ren, Z. Mei, M. Gu and F. Pan, *Catal. Sci. Technol.*, 2019, **9**, 803-810.